# Yb-doped $RbTiOPO_4$ crystals for self-frequency doubling applications**

Joan J. Carvajal, Rosa M. Solé, Josefina Gavaldà, Jaume Massons, Patricia Segonds, Benoît Boulanger, Alain Brenier, Georges Boulon, J. Zaccaro, Magdalena Aguiló and Francesc Díaz*

Interest has increased in developing compact green laser sources for high-density optical data storage and display applications, such as colour projection, laser printing, medicine, biofluorescence, underwater communications, stereo lithography and photodynamic therapy[1] since the promising investigations into wide-gap diode lasers,[2,3] harmonic generation by phase matching in nonlinear crystals,[4] quasi-phasematching in bulk,[5] optical fibres and other waveguides,[6] and upconversion lasers in crystals[7] and fibres.[8] Using non linear optical processes such as frequency doubling in laser materials is very promising for the realization of these compact all-solid-state laser sources, but so far only a few non linear crystals doped with $Nd^{3+}$ have been used to do this:[1] $LiNbO_3$ (LNB), $LaBGeO_5$, $Ba_2NaNb_5O_{15}$, $\beta$-$Gd_2(MoO_4)_3$, $YAl_3(BO_3)_4$ (YAB), $CaY_4O(BO_3)_3$ (YCOB) and $CaGd_4O(BO_3)_3$.

More recently, $Yb^{3+}$ also appeared as a promising ion in the same range of emission wavelength and several highly efficient Yb-lasing in self-frequency doubling materials have been reported in YAB, LNB and YCOB. [1] This is due to a very simple energy level scheme of $Yb^{3+}$ which is made up of only two levels: the $^2F_{7/2}$ ground state and the $^2F_{5/2}$ excited state. Moreover, there is no excited state absorption to reduce the effective laser cross-section, no up-conversion, no concentration quenching and no absorption in the green. Finally, the intense $Yb^{3+}$ absorption lines are well suited for laser diode pumping near 980 nm from high-power

* Mr. J. J. Carvajal, Dr. R. M. Solé, Dr. Jna. Gavaldà, Dr. J. Massons, Dr. M. Aguiló, Dr. F. Díaz,
Física i Cristal·lografia de Materials, Universitat Rovira i Virgili, Pl. Imperial Tarraco, 1, 43005, Tarragona (Spain)
E-mail : diaz@quimica.urv.es
Dr. P. Segonds, Dr. B. Boulanger
Laboratoire de Spectrométrie Physique, Université Joseph Fourier, Sant Martin d'Hères (France)
Dr. A. Brenier, Dr. G. Boulon
Laboratoire de Physico-Chimie de Matériaux Luminescents, Université Claude Bernard, Villeurbane (France)
Dr. J. Zaccaro
Laboratoire de Cristallographie, CNRS, Grenoble (France)
** This research is supported by the CIRIT (2001SGR317) and CICyT (MAT2002-04603-C05-03 and FIT-070000-2002-461). J.J. Carvajal gratefully acknowledges the grant from the Catalan Government (2000FI 00633)

InGaAs diode lasers and the small Stokes shift between absorption and emission reduces the thermal loading of the material during the laser operation.

Since $KTiOPO_4$ (KTP) has been established as unique inorganic non linear crystal for frequency conversion applications[9-12] and as the material of choice for frequency doubling Nd-lasers at 1 μm radiation,[9,13-15] literature reports doping of KTP with lanthanide elements using different techniques. [16] However, the concentration achieved in bulk crystals is limited to $5 \times 10^{17}$ - $6 \times 10^{18}$ ions·cm$^{-3}$, which is weak. Higher concentrations of lanthanide ions have been obtained by thermal diffusion of $Ln_2O_3$ layers deposited by laser ablation on KTP surfaces,[17] or implantation and ion beam mixing,[18,19] but damage caused to the sample, the degradation of its surface and the deposition of $LnPO_4$ phases restrict the use of such techniques.

On the other hand, substituting $K^+$ with $Rb^+$ in the KTP structure lead to similar non linear properties for $RbTiOPO_4$ (RTP). Moreover, using $Nb^{5+}$ as codopant in RTP seems to be a good way to obtain a high enough concentration of $Ln^{3+}$ to produce an efficient laser emission. [20,21]

In this communication, we report for the first time the crystal growth of $RbTiOPO_4$ doped with (Nb,Yb). We have performed the spectroscopic characterization: we show absorption and emission spectra and second harmonic generation measurements. The results predict a favourable disposition for the use of Yb-doped RTP crystals as self-frequency doubling laser materials.

We obtained single crystals of high optical quality with a concentration of $Yb^{3+}$ of $1.96 \times 10^{20}$ ions·cm$^{-3}$, emitting at around 1μm. Like KTP and isomorphs, this material crystallizes in the orthorhombic system, with the space group of symmetry $Pna2_1$. Figure 1 shows a single crystal of $RbTi_{0.935}Nb_{0.043}Yb_{0.022}OPO_4$ (RTP:(Nb,Yb)) grown by the top-seeded solution growth (TSSG) and a schematic view of its morphology.

Electron probe microanalysis (EPMA) reports that the concentration of $Yb^{3+}$ is the highest ever obtained in a bulk crystal of the KTP family. Figure 2 shows the homogeneity of distribution of Nb and Yb along two of the three different crystallographic directions. The concentration of doping ions decreases the closer we are to the crystal seed, because their distribution coefficients are less than one. Then, during the growth process, the solution becomes richer in these ions and their incorporation into the crystal increases. However, there were no substantial differences in the absorption and emission spectra of $Yb^{3+}$ taken at different parts of the crystal. $Nb^{5+}$ and $Yb^{3+}$ in these crystals are expected to substitute $Ti^{4+}$ in the structure, as with RTP:(Nb,Er) crystals.[23,24] The smaller ionic radius of $Yb^{3+}$ with respect to

$Er^{3+}$ in an octahedrical environment,[25] which is closer to that of $Ti^{4+}$, reinforces this assumption.

The absorption and emission spectra around 1 μm of the RTP:(Nb,Yb) crystal are shown in Figures 3 and 4. The absorption spectra were recorded with the electrical field of the incident light parallel to the ***a***, ***b*** and ***c***-axis, and were compared with Raman spectra to distinguish the vibronic and electronic contributions. The three expected peaks, corresponding to the splitting of the $^2F_{5/2}$ multiplet, were found around 903, 955 and 972 nm. The absorption peaks at 903 and 972 nm were the strongest. The absorption spectra show a large splitting of the $^2F_{5/2}$ sublevels of about 70 nm, which is one of the largest crystal field, comparable with Yb-doped fluoroapathites.[26] This large splitting indicates that a broadband fluorescence can be obtained, which is interesting for tunability and subpicosecond-pulse generation applications in the visible and in the infrared domains. The value of the absorption cross section ($\sigma_a$) depended strongly on the polarization of the incident light as it is shown in Figure 3. This means that the number and positions of the absorption peaks are independent of the polarization but that the intensity of a gien peal can depend on the polarization. We found that the two external peaks invert their intensity in the spectra parallel to the ***b***- and ***c***-axes and that the spectrum collected parallel to the ***a***-axis is less intense than the other ones. The emission spectra shown in Figure 4 were obtained by exciting the sample at 972 nm, and were recorded with the electrical field of the emitted light parallel to the ***a***-, ***b***- and ***c***-axes. These spectra show the typical emission of $Yb^{3+}$ at around 1 μm wavelength and confirm the broadband fluorescence expected from the large splitting of the absorption spectra, which is very important for population inversion in the laser emission process. The peaks in the measured spectrum correspond to the emission from the excited $^2F_{5/2}$ manifold to the four sublevels of the ground state manifold $^2F_{7/2}$ located at 972, 1025, 1051 and 1071 nm. The intensities of the spectra again depended on the polarization of the emitted signal in this order: ***c*** > ***b*** > ***a***.

We used the Früchbauer-Ladenburg method to calculate the $Yb^{3+}$ emission cross sections $\sigma_{a,b,c}$ in polarization parallel to ***a***-, ***b***- and ***c***- axes in the $RbTi_{0.935}Nb_{0.043}Yb_{0.022}OPO_4$ crystal, leading to the following expression:

$$\sigma_{a,b,c}(\lambda) = \frac{\lambda^4 I_{a,b,c}(\lambda)}{8\pi n^2 c \tau_f \int \frac{I_a + I_b + I_c}{3} d\lambda} \qquad \text{Eq.1}$$

where $\lambda$ is the wavelength, $I_{a,b,c}$ is the ***a***-, ***b***-, ***c***-polarized emission spectrum, $n$ is the refractive index, $c$ is the vacuum speed of the light, and $\tau_f$ is the spontaneous fluorescence time.

It is important to accurately measure the excited-state lifetime as a further step to characterising a laser material. It is well known that radiation trapping and total internal reflection can strongly affect the measured lifetimes, related with the reabsorption of the initial emission by ions in the ground state, followed by reemission and lengthening of the measured lifetime. However, these effects can be neglected in our crystals because the concentration of $Yb^{3+}$ is not extremely high. We determined the fluorescence lifetime $\tau_f$ by collecting the decay of the luminescence intensity of the strongest peak of the luminescence spectra. The fluorescence decay is characterized by single exponential behaviour and has a quite long value of 2.2 ms. Such a long lifetime is favourable to get a high inversion of population under CW pumping.

We measured the fundamental wavelength of type II angular non critical phase-matching (NCPM) for second harmonic generation (SHG), $\lambda_{NCPM}$, of RTP samples doped in different concentration with Nb and/or Yb. According to the crystallographic orientation of these crystals we were able to study only the $x$-principal axis which corresponds to the ***a***-crystallographic one. The relation between the involved principal refractive indices is then:

$$n_y\left(\frac{\lambda_{NCPM}}{2}\right) = \frac{n_y(\lambda_{NCPM}) + n_z(\lambda_{NCPM})}{2} \qquad \text{Eq. 2}$$

The values of $\lambda_{NCPM}$ are summarized in Table 1. It is not reasonable to establish a precise rule of $\lambda_{NCPM}$ and of the principal refractive indices $n_y$ and $n_z$ with the concentration from these measurements. Nevertheless, it appears clearly that the increasing of $Yb^{3+}$ concentration leads to an increasing of $\lambda_{NCPM}$, so that $RbTi_{0.993}Yb_{0.007}OPO_4$ has exactly the same NCPM wavelength than $KTiOAsO_4$ (KTA). [27] We also verified that all the samples studied exhibit a conversion efficiency of the order of that of RTP.

In conclusion, we have successfully grown for the first time high optical quality crystals of $RbTiOPO_4$ doped with $Yb^{3+}$. These crystals show a broadband fluorescence around 1μm, which is interesting for tunability and sub-picosecond-pulse generation applications in the infrared. The long radiation lifetime of $Yb^{3+}$ in these crystals is also favourable for achieving efficient power laser emission in this region. Their good non linear optical properties are close to those of RTP,[28] KTP,[27] and KTA.[26] Thus these crystals are good candidates for self-frequency doubling applications. We are working on a future research line which can match with the possibility of co-dope RTP with $Er^{3+}$ and $Yb^{3+}$: it is of great importance in optical amplifiers for telecommunication $Er^{3+}$ is pumped indirectly via $Yb^{3+}$.

## Experimental

*Crystal growth*: Briefly, single crystals of RTP:(Nb,Yb) were grown by the TSSG-slow-cooling technique using a vertical tubular furnace controlled by a Eurotherm 902 controller/programmer connected to a thyristor.[21] Solutions of about 160 g were prepared by mixing suitable amounts of $Rb_2CO_3$, $NH_4H_2PO_4$, $TiO_2$, $Nb_2O_5$ and $Yb_2O_3$, used as initial reagents, in a Pt crucible of 125 $cm^3$. These reagents were decomposed by heating them until the bubbling of $NH_3$, $H_2O$ and $CO_2$ was complete and maintaining the solution at a temperature of about 50-100 K above the expected saturation temperature for 3-5 h to homogenise them. The crystals were grown on RTP:(Nb,Yb) seeds of 5.0 × 1.5 × 5.0 mm along $\boldsymbol{a} \times \boldsymbol{b} \times \boldsymbol{c}$ crystallographic axes respectively. The ***c***-axis was oriented perpendicular to the surface of the solution, displaced 4-5 mm from the rotation axis, and fixed in a growth device that included a platinum turbine to also stir the solution.[20] The ***a***-axis of the two seeds used in every growth experiment was always placed in the radial direction of the rotation movement. We determined the saturation temperature from the growth or dissolution of the seeds in contact with the surface of the solution. The rotation was kept constant at 65 rpm in all experiments. When the growth process was complete, we slowly removed the crystals from the solution and decreased the temperature of the furnace to room temperature to minimise any thermal stress.

*Measuring techniques*: We analysed the concentration of dopants by EPMA operating in wavelength dispersive mode in a CAMECA SX-50 electron microprobe. The crystallographic orientation was realized by an X-ray automatic diffractometer. Optical absorption was performed with a Perkin-Elmer Lamda 900 Spectrophotometer. A Glan-Thompson quartz polarizer located before the sample was used in order to eliminate the possible polarization induced by the optical components of the spectrophotometer and to ensure that we were working only with a polarized component of the incident light. Luminescence spectra were recorded by exciting the samples at 972 nm with a Laser Analytical Systems dye laser that delivered excitation pulses of 10 ns in duration and at a repetition rate of 10 Hz. This luminescence was analysed with an HRS2 Jovin-Yvon monochromator, with a focal length of

70 cm and equipped with 1 μm blazed grating, and detected by a Hamamatsu R1767 photomultiplier. The radiative lifetime was measured with a LeCroy 9400 digital oscilloscope. The type II angular non critical phase-matching (NCPM) fundamental wavelengths for second harmonic generation (SHG) were measured by illuminating the samples with a focused tunable beam. The laser source was a Continuum Panther OPO pumped by a Continuum SLI-10 YAG:Nd laser which is 10 Hz-repetition rate and 4 ns-FWHM pulse duration. This emitted between 410 and 2550 nm. An achromatic half-wave plate was used to adjust the polarization of the incident beam to ensure type II phase-matching. The wavelength of the OPO was controlled by a CHROMEX 250 SM scanning monochromator.

**References**


[1] A. Brenier, *J. Lumin.*, **2000**, *91*, 121

[2] M.A. Haase, J. Qiu, J.M. DePuydt, H. Cheng, *Appl. Phys. Lett.*, **1991**, *59*, 1272

[3] H. Jeon, J. Ding, W. Patterson, A.V. Nurmikko, W. Xie, D.C. Grillo, M. Kobayashi, R.L. Gunshor, *Appl. Phys. Lett.,* **1991**, *59*, 3619

[4] L. Goldberg, M.K. Chun, *Appl. Phys. Lett.*, **1989**, *47*, 218

[5] J. Hellström, G. Karlsson, V. Pasiskevicius, F. Laurell, *Opt. Lett.*, **2001**, *26*, 352

[6] A. Feisst, P. Koidl, *Appl. Phys. Lett.*, **1985**, *47*, 1125

[7] L.F. Johnson, H.J. Guggenheim, *Appl. Phys. Lett.*, **1971**, *19*, 44

[8] J.Y. Allain, M. Monerie, H. Poignant, *Electron. Lett.*, **1990**, *26*, 166

[9] F.C. Zumsteg, J.D. Bierlein, T.E. Gier, *J. Appl. Phys.*, **1976**, *47*, 4980

[10] G.D. Stucky, M.L.F. Phillips, T.E. Gier, *Chem. Mater.*, **1989**, *1*, 492

[11] M.N. Satyanarayan, A. Deepthy, H.L. Bhat, *Critical Reviews in Solid State and Materials Sciences*, **1999**, *24*, 103

[12] M.E. Hagerman, K.R. Poeppelmeier, *Chem. Mater.*, **1995**, *7*, 602

[13] T.Y. Fan, C.E. Huang, B.Q. Hu, R.C. Eckhardt, Y.X. Fan, R.L. Byer, R.S. Feigelson, *Appl. Opt.*, **1987**, *26*, 2391

[14] J.D. Bierlein, H. Vanherzeele, *J. Opt. Soc. Am. B*, **1989**, *6*, 622

[15] J.C. Jacco, *SPIE Int. Soc. Opt. Eng.*, **1988**, *93*, 968

[16] C. Zaldo, M. Rico, F. Díaz, J.J. Carvajal, *Opt. Mat.*, **1999**, *13*, 175

[17] M.J. Martin, C. Zaldo, M.F. Da Silva, J.C. Soares, F. Díaz, M. Aguiló, *J. Phys. Condens. Matter.*, **1997**, *9*, L465

[18] L. Zhang, P.J. Chandler, P.D. Townsend, P.A. Thomas, *Electron. Lett.*, **1992**, *28*,1478

[19] K.M. Wang, B.R. Shi, P.J. Diong, W. Wang, W.A. Landford, Z. Zhou, Y.G. Liu, *J. Mater. Res.*, **1996**, *11*, 1333

[20] J.J. Carvajal, V. Nikolov, R. Solé, Jna. Gavaldà, J. Massons, M. Rico, C. Zaldo, M. Aguiló, F. Díaz, *Chem. Mater.*, **2000**, *12*, 3171

[21] J.J. Carvajal, V. Nikolov, R. Solé, Jna. Gavaldà, J. Massons, M. Aguiló, F. Díaz, *Chem. Mater.*, **2002**, *14*, 3136

[22] J.J. Carvajal, R. Solé, Jna. Gavaldà, J. Massons, M. Aguiló, F. Díaz, *Cryst. Growth & Design*, **2001**, *1*, 479

[23] J.J. Carvajal, J.L. García-Muñoz, R. Solé, Jna. Gavaldà, J. Massons, M. Aguiló, F. Díaz, *J. Solid State Chem.*, **2003**, *171*, 257

[24] J.J. Carvajal, J.L. García-Muñoz, R. Solé, Jna. Gavaldà, J. Massons, X. Solans, F. Díaz, M. Aguiló, *Chem. Mater.*, in press.

[25] R.D. Shannon, *Acta Crystallogr.*, **1976**, *A32*, 751

[26] L.D. Deloach, S.A. Payne, L.K. Smith, W.L. Kway, W.F. Krupke, *J. Opt. Soc. Am. B*, **1994**, *11*, 269

[27] B. Boulanger, J.P. Fève, G. Marnier, B. Ménaert, *Pure Appl. Opt.*, **1998**, *7*, 239

[28] Y. Guillien, B. Ménaert, J.P. Fève, P. Segonds, J. Douady, B. Boulanger, O. Pacaud, *Appl. Matter.*, **2003**, *22*, 155

**Figure Captions**

Fig. 1. Single crystal of $RbTi_{0.93}Nb_{0.05}Yb_{0.02}OPO_4$ grown by the TSSG technique and schematic view of its morphology.

Fig. 2. Variation of the concentration of $Yb^{3+}$ (upper value) and $Nb^{5+}$ (lower value) in atom % along the ***b*** and ***c*** crystallographic directions in an internal surface of a $RbTi_{0.93}Nb_{0.05}Yb_{0.02}OPO_4$ crystal grown with a seed oriented with the ***c*** crystallographic direction normal to the surface of the solution of growth.

Fig. 3. Absorption spectra of $Yb^{3+}$ in the $RbTi_{0.93}Nb_{0.05}Yb_{0.02}OPO_4$ crystal, corresponding to the $^2F_{7/2} \rightarrow {}^2F_{5/2}$ transitions.

Fig. 4. Emission spectra of $Yb^{3+}$ in the $RbTi_{0.93}Nb_{0.05}Yb_{0.02}OPO_4$ crystal, corresponding to the $^2F_{5/2} \rightarrow {}^2F_{7/2}$ transitions.

Table 1. Type II angular non critical phase-matching (NCPM) SHG fundamental wavelength, $\lambda_{NCPM}$, as a function of chemical composition.

| Sample | $\lambda_{NCPM}$ ± 1 nm |
|---|---|
| $RbTiOPO_4$ | 1144 |
| $RbTi_{0.942}Nb_{0.058}OPO_4$ | 1101 |
| $RbTi_{0.993}Yb_{0.007}OPO_4$ | 1148 |
| $RbTi_{0.935}Nb_{0.043}Yb_{0.022}OPO_4$ | 1119 |

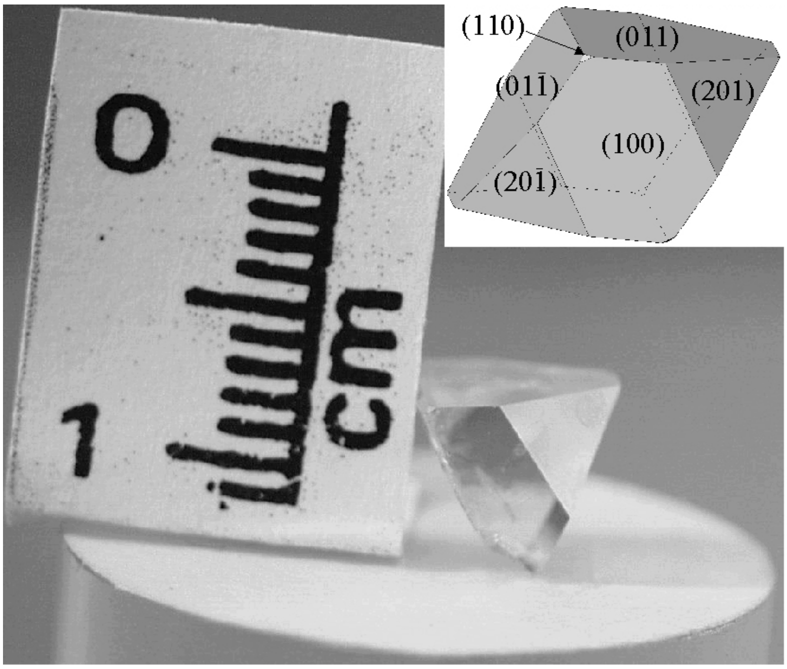
(110)
(011)
(01$\bar{1}$)
(201)
(100)
(20$\bar{1}$)
0
1
cm

Fig. 1

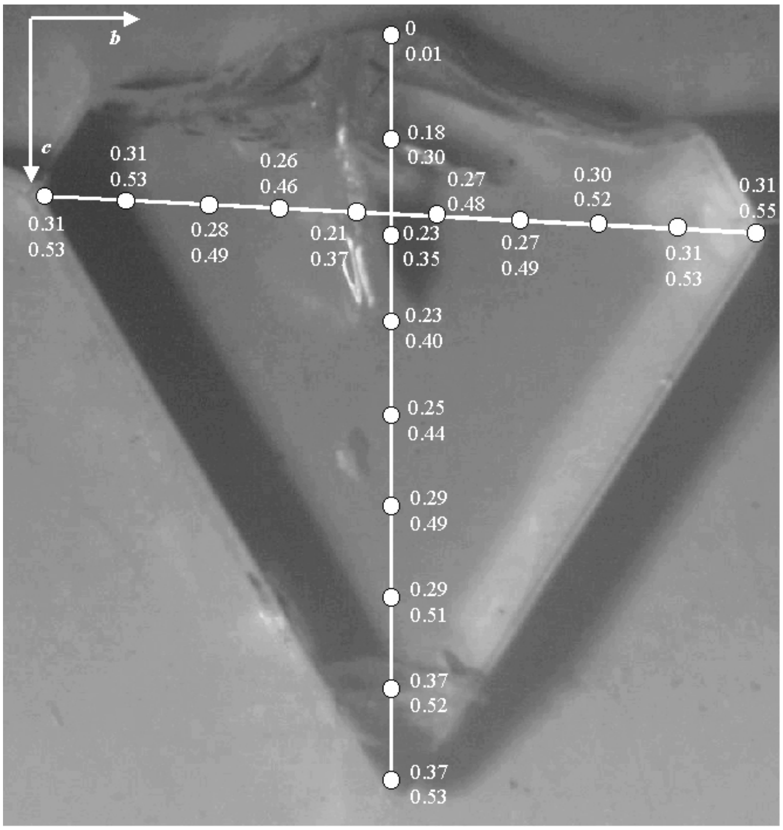
b
c
0
0.01
0.18
0.30
0.31
0.53
0.26
0.46
0.27
0.48
0.30
0.52
0.31
0.55
0.31
0.53
0.28
0.49
0.21
0.37
0.23
0.35
0.27
0.49
0.31
0.53
0.23
0.40
0.25
0.44
0.29
0.49
0.29
0.51
0.37
0.52
0.37
0.53

Fig. 2

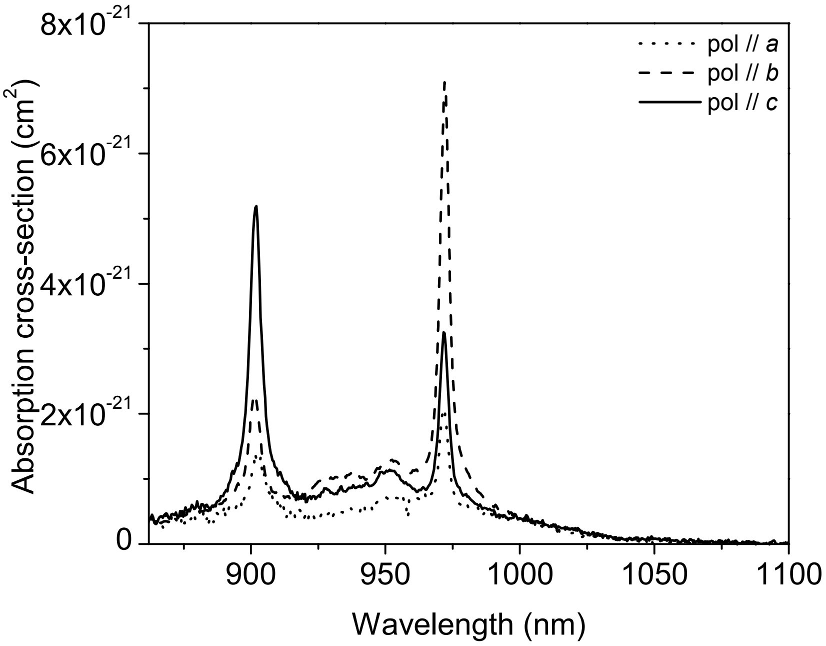

8x10$^{-21}$
6x10$^{-21}$
4x10$^{-21}$
2x10$^{-21}$
0
Absorption cross-section (cm$^2$)
900
950
1000
1050
1100
Wavelength (nm)
pol // *a*
pol // *b*
pol // *c*


Fig. 3

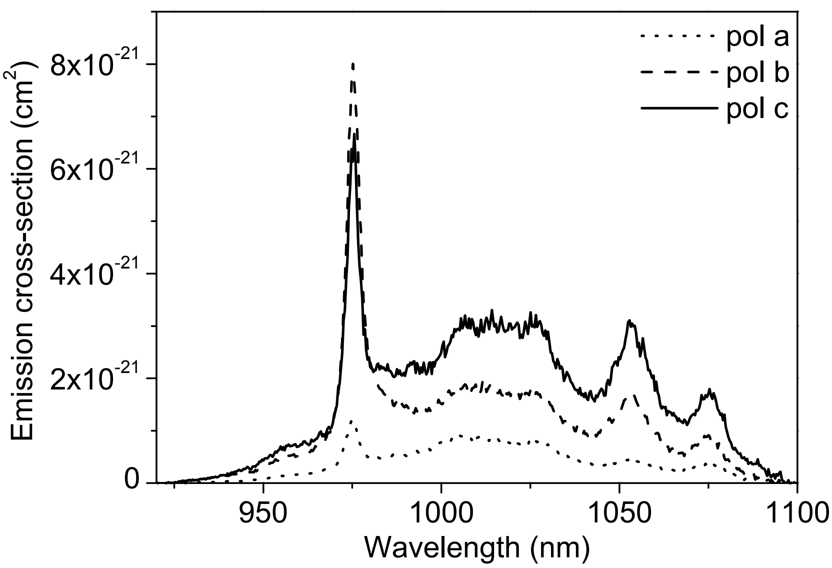

8x10$^{-21}$
6x10$^{-21}$
4x10$^{-21}$
2x10$^{-21}$
0
Emission cross-section (cm$^2$)
950
1000
1050
1100
Wavelength (nm)
pol a
pol b
pol c


Fig. 4